Supporting Information

A Boronic Acid-based Neutral Two-Component Ferroelectric for Piezoelectric Energy Harvesting and Charge-Storage Applications

Supriya Sahoo,[a] Nilotpal Deka,[a] Vikash Kushwaha,[a] Vinayak B. Gadagin,[a] Jan K. Zaręba,*[b] and Ramamoorthy Boomishankar*[a]

[a]Department of Chemistry and Centre for Energy Science, Indian Institute of Science Education and Research, Pune, Dr. Homi Bhabha Road, Pune – 411008, India
[b]Institute of Advanced Materials, Wrocław University of Science and Technology, 50-370 Wrocław, Poland

Table of contents

EXPERIMENTAL SECTION

General Remarks

2-aminopyrimidine and 4-formylphenyl boronic acid were purchased from BLD Pharma and were used without further purification. The thermogravimetric analyses were performed using the PerkinElmer STA-6000 analyzer at a heating rate of 10 °C/min in a nitrogen atmosphere. Differential scanning calorimetry (DSC) measurements were performed on a TA Q20 differential scanning calorimeter with heating and cooling rates of 10 °C/min under the nitrogen atmosphere. Melting point analyses were done using a Buchi M-560 melting point apparatus. The powder X-ray diffraction (PXRD) data were measured in the 2θ range of 5 to 50° on a Bruker-D8 Advance X-ray diffractometer.

Synthesis of AP·FPBA Co-crystal:

The compound **AP·FPBA** was synthesized by grinding 2-aminopyrimidine and 4-formylphenyl boronic acid in a 1:1 ratio. The powdered mixture was then dissolved in methanol, and plate-like crystals of **AP·FPBA** were obtained after a week. Yield: 84 %. Anal. Calcd. for $C_{11}H_{12}BN_3O_3$: C 53.92; H 4.94; N 17.15. Found: C 53.82; H 4.67; N 17.18.

Single Crystal X-ray Diffraction Analysis:

The single-crystal X-ray diffraction data for **AP·FPBA** were collected at 120 K and 298 K by using the Mo K_α radiation (λ = 0.71073 Å) on a Bruker Smart Apex Duo diffractometer. Direct methods were used to solve the crystal structure, and then refinements were done by full-matrix least-squares against F^2, utilizing SHELXL-2014/7 integrated into the Apex 3 program.[54] All non-hydrogen atoms were refined anisotropically.[55] The positions of the hydrogen atoms were determined geometrically to their parent atoms. The structural illustrations of **AP·FPBA** were made by utilizing the DIAMOND-3.1 software.

Hirshfeld Surface Analysis:

To visualize the various types of interactions, normalized contact distance (d_{norm}), shape index, and curvedness present on the Hirshfeld surface of **AP·FPBA**, the Crystal Explorer 3.1 program was utilized. For this purpose, the single-crystal X-ray crystallographic information file (CIF) was employed. These interactions were depicted as 3D color mapping images, with intense interactions represented by red, medium by blue, and weak by white. The Hirshfeld surface **AP·FPBA** was color-coded using different colors to generate diverse surface color mappings. Additionally, 2D fingerprint plots were constructed for **AP·FPBA**. These plots are histograms that compile the distances of given atoms closest to the interior (d_i) and exterior (d_e) of the generated Hirshfeld surface. The different contours in the 2D fingerprint plots were represented by blue and grey colors, illustrating the various molecular interaction types.

X-ray Photoelectron Spectroscopy:

Thermo Fisher Scientific UK Model K alpha+ spectrometer operating at 72 W power was used to analyze the X-ray photoelectron spectroscopy (XPS) spectrum of **AP·FPBA**. The monochromatic Al K_α anode (1486.6 eV) was used as the X-ray source. The sample loading and analyzer chambers were kept at vacuum pressures of 1.2×10^{-8} mbar and 2×10^{-9} mbar, respectively. 400 μm spot-size micro-focused X-ray sources were used for data acquisition. A pass energy of 200 eV was used for the high-resolution survey scan, while a 50 eV pass energy was used to record individual core-level spectra. Charge compensation, maintained through ultra-low energy co-axial electron and Ar+ ion beams, remained active during spectral acquisition. The binding energies of the different elements in the sample were determined by energy calibration using the C1s standard value of 284.6 eV. During the data collection process, the spectrometer base pressure was maintained at or above 5×10^{-9} mbar and 1×10^{-7} mbar with the flood cannon activated. Avantage software was utilized to handle raw data with an instrument resolution of ± 0.1 eV. Smart background subtraction was applied for peak fitting.

Nonlinear Optical Measurements:

Nonlinear optical (NLO) experiments were performed using a laser system employing a wavelength-tunable Topaz Prime Vis-NIR optical parametric amplifier (OPA) pumped by a Coherent Astrella Ti:Sapphire regenerative amplifier providing femtosecond laser pulses (800 nm, 75 fs) at a 1 kHz repetition rate. The output of OPA was set to 1300 nm and the laser fluence at samples was 0.19 mJ/cm^2.

To perform a Kurtz-Perry test, the single crystals **AP·FPBA** and reference potassium dihydrogen phosphate (KDP) were crushed with a spatula and sieved through an Aldrich mini-sieve set. Microcrystals of size fraction 125–177 μm were collected. In the proceeding step, size-graded **AP·FPBA** and KDP samples were fixed between microscope glass slides to form tightly packed, uniform layers, which were then sealed and mounted to the horizontally aligned sample holder. For this purpose, no refractive index matching oil was used. Under the same excitation conditions, the SHG signal was collected for **AP·FPBA** and KDP for 2000 ms and 200 ms, respectively.

The employed measurement setup operates in the reflection mode. Specifically, the laser beam delivered from the regenerative amplifier passed through a 5 mm aperture and was directed onto the sample at 45° to its surface. Emission collecting optics consisted of a Ø25.0 mm plano-convex lens of focal length 25.4 mm mounted to the 400 μm 0.22 NA glass optical fiber and was placed along the normal to the sample surface. The distance between the collection lens and the sample was equal to 30 mm. The spectra of SHG responses were recorded by an Ocean Optics Flame T fiber-coupled CCD spectrograph with a 200 μm entrance slit. Scattered pumping radiation was suppressed with the use of a Thorlabs 750 nm short-pass dielectric filter (FESH0750).

Ferroelectric and Dielectric Measurements:

The *P-E* hysteresis loop measurements for **AP·FPBA** were carried out on its drop-casted thin film on an Indium tin oxide (ITO)-coated glass surface, and Gallium Indium eutectic was used as the top contact. The ferroelectric polarization vs. electric field (*P-E*) measurements were conducted using the aixACCT TF-2000E model hysteresis loop analyzer by applying the dynamic leakage current compensation (DLCC) mode to reduce the contributions from non-hysteretic components of the loop. The leakage currents were recorded dynamically during the hysteresis loop measurements. The ferroelectric fatigue measurements were performed for 10^6 cycles under the same DLCC conditions.

For the dielectric permittivity measurements, a powder-pressed pellet of **AP·FPBA** was used. The measurements were performed using the Solartron Analytical Impedance Analyzer model 1260, which was coupled with a Dielectric Interface 1296A. The equipment was operated with a Janis 129610A cryostat sample holder and a Lakeshore 336 model temperature controller.

Piezoresponse Force Microscopy Characterizations:

The piezo- and ferroelectric properties of the crystal film of material **AP·FPBA** prepared on ITO (Indium tin oxide) coated glass surface were studied using PFM measurements conducted with the Asylum Research MFP-3D atomic force microscopy (AFM) system. Contact mode AFM experiments were carried out using RMN-12PT300B cantilever probes, which had a spring constant of 1.12 N m^{-1} and a tip diameter of less than 8 nm, to measure the piezoresponse of the crystal films. PFM data was obtained through vertical-PFM experiments, wherein an AC voltage was applied to the conductive AFM tip while the bottom electrode remained grounded. The PFM images were collected at a resonance frequency of 300 +/- 20 kHz, with an applied bias of 100 V. Additionally, PFM phase and amplitude contrast were recorded using dual AC resonance tracking (DART) mode PFM.

Direct Piezoelectric Coefficient (d_{33}) Measurements:

The piezoelectric charge coefficient (d_{33}) of **AP·FPBA** was measured on its pressed pellet (5 mm diameter, 1 mm thickness) using the "Berlincourt" method. The pressed pellets were poled with a 12 kV/cm field for 20 min. The APC International wide-range d_{33} tester, with an operating force frequency of 110 Hz and an amplitude of 0.25 N, was utilized. The electrical contacts were made with a silver conductive paste.

Piezoelectric Energy Harvesting Measurements:

A periodic impact instrument, customized to operate at an impact force of 21 N and frequency of 10 Hz, was used to carry out the mechanical energy harvesting experiments. The output voltages and currents were measured using a Tektronix 2024 Mixed Signal Oscilloscope. The devices under test (**AP·FPBA**) had a thickness of approximately 1 mm and an active area of 100 mm^2.

Capacitance Calculations and Charge Storage Measurements of the device:

We calculated the capacitance values of **AP·FPBA** on its thin films of dimensions 2.2 × 2.2 mm^2 and 0.13 mm thickness. For charge storage measurements, a film of **AP·FPBA** was prepared by drop casting method. The thin-film substrate was prepared by preparing a 60 mg ml^{-1} suspension of **AP·FPBA** in hexane and drop casting onto a pre-cleaned 25 × 25 mm^2 ITO-coated glass substrate at room temperature. The cured film was measured to have a thickness of 0.13 mm. For electrical contacts, 50 nm of Cr/100 nm Au was deposited on the thin film top surface of **AP·FPBA** via sputtering through a shadow mask to create a square top electrode of 2.2 × 2.2 mm^2 area. A two-electrode probe station was used to contact the bottom and top electrodes of the device. Voltage pulses were applied through a home-built signal generator and the resultant voltage signals from the thin-film samples were measured by a Keithley digital multi-meter DMM7510 7.5.

To calculate the capacitance of the **AP·FPBA** thin films, the impedance values were taken from its compacted bulk pellet using the Solartron Analytical Impedance Analyzer model 1260. The following correlations have been applied to calculate the capacitance values of the thin films from the bulk impedance values.
The impedance *Z* of the pellet is given by,
$$Z = Z_R - jZ_c$$
Where Z_R is the real part corresponding to the purely resistive behaviour.
Z_C is the purely capacitive behaviour at a given frequency (*f*).
$$Z_c = \frac{1}{j\omega C}$$
$$Z_c = \frac{1}{j2\pi f C}$$
$$C = \frac{1}{2\pi f |Z_c|}$$
ε_1, d_1 (1.26 mm), C_1, A_1 (78.25 mm^2) are the relative permittivity, thickness, capacitance, and area of the compacted pallet, respectively and ε_2, d_2 (0.13 mm), C_2, A_2 (4.8 mm^2) are the corresponding relative permittivity, thickness, capacitance, and area of the device.
$$Z_c = \frac{1}{2\pi f C_1} \rightarrow C_1 = \frac{1}{2\pi f Z_c}$$

So, the relative permittivity of the pallet in terms of capacitance is given below:

$$\varepsilon_1 = C1 \times \frac{d1}{A2 \times \varepsilon_0}$$

The dielectric constant and proportionality relation to the relative permittivity (ε_2) of the device is given as

$$\varepsilon_2 = \varepsilon_1 \times \frac{A2 \times d1}{A1 \times d2}$$

Subsequently, the capacitance value of the thin-film device can be calculated by the expression given below.

$$C2 = \varepsilon_0 \times \varepsilon_2 \times \frac{A2}{d2}$$

Table S1. X-ray Crystallographic data for **AP·FPBA**.

Crystallographic details	AP·FPBA (150 K)	AP·FPBA (298 K)
Chemical formula	$C_{11}H_{12}BN_3O_3$	$C_{11}H_{12}BN_3O_3$
Formula weight (g/mol)	245.05	245.05
Temperature (K)	150(2)	298(2)
Crystal system	Orthorhombic	Orthorhombic
Space group	$Pca2_1$	$Pca2_1$
a (Å); α (°)	11.140(2); 90	11.316(7); 90
b (Å); β (°)	12.094(2); 90	12.087(7); 90
c (Å); γ (°)	17.656(4); 90	17.975(11); 90
V (Å³); Z	2378.8(8); 8	2459(3); 8
ρ (calc.) g cm^{-3}	1.368	1.324
μ (Mo K$_\alpha$) mm^{-1}	0.100	0.097
$2\theta_{max}$ (°)	50.054	57.014
R(int)	0.2387	0.1266
Completeness to θ	100	100
Data / param.	4207/331	6049/327
GOF	1.026	0.940
R1 [F>4σ(F)]	0.0619	0.0546
wR2 (all data)	0.1021	0.1441
max. peak/hole (e.Å^{-3})	0.278/ -0.249	0.165/-0.195
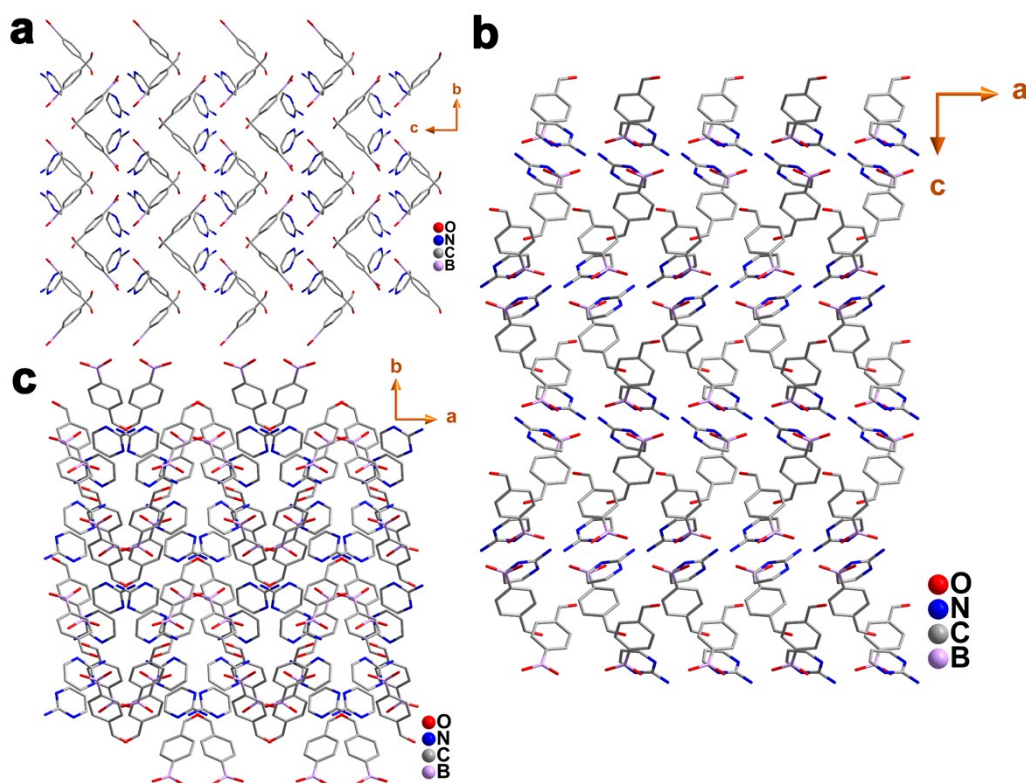
Figure S1. Packing diagrams of **AP·FPBA** along (a) *a*-axis (b) *b*-axis and (c) *c*-axis at 150 K.

Table S2. Hydrogen bonding parameters for **AP·FPBA** at 150 K.

D-H···A	d(H···A) Å	d(D-A) Å	<(DHA)	Symmetry transformations to generate equivalent atoms
N(11)-H(11A)···O53	2.0928(37)Å	2.9557(61) Å	166.668(337)	1.5-x, -1+y, 0.5+z
N(11)-H(11B)···O52	2.3459(43)Å	3.0601(71) Å	138.323(378)	1-x, 1-y, 0.5+z
O52- H(52)···N(12)	1.9327(50)Å	2.7571(63) Å	166.898(291)	1.5+x, 1+y, -0.5+z
O63-H(63)···N(13)	1.9422(55)Å	2.7340(69) Å	156.602(323)	x, y, z
N(21)-H(21A)···O62	2.1270(44)Å	2.9647(71) Å	158.832(337)	0.5+x, 1-y, z
N(21)-H(21B)···O63	2.0886(37)Å	2.9553(61) Å	167.414(336)	x, y, z
O53-H(53)···N(22)	2.0187(54)Å	2.8099(68) Å	156.725(316)	1.5-x, y, -0.5+z
O62-H(62)···N(23)	1.9591(50)Å	2.7799(62) Å	165.221(291)	-0.5-x, 1-y, z
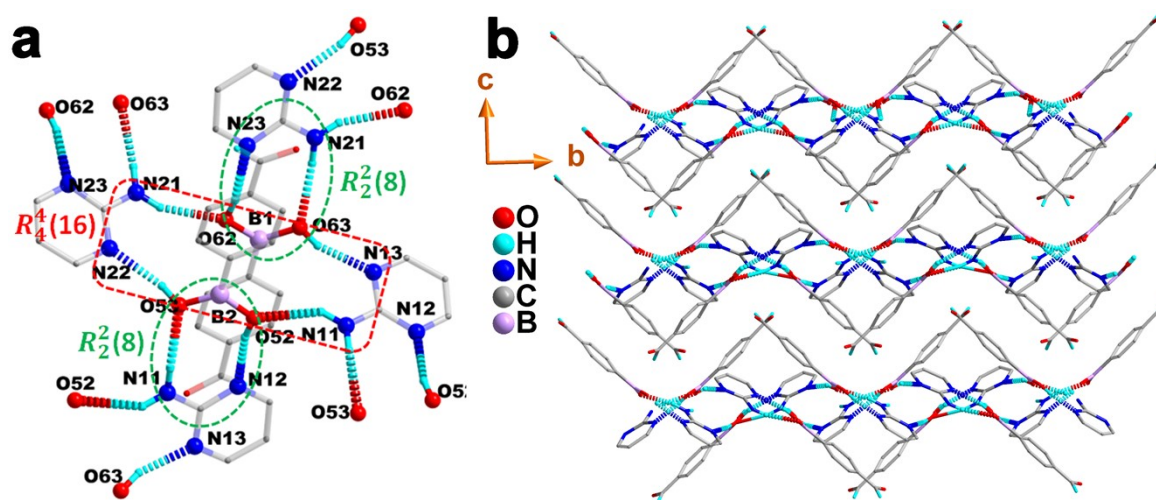
Figure S2. The O···H hydrogen bonding interactions in **AP·FPBA** at 150 K. (a) Stacked H-bonded 2D-sheets of **AP·FPBA** growing along *b*-axis.
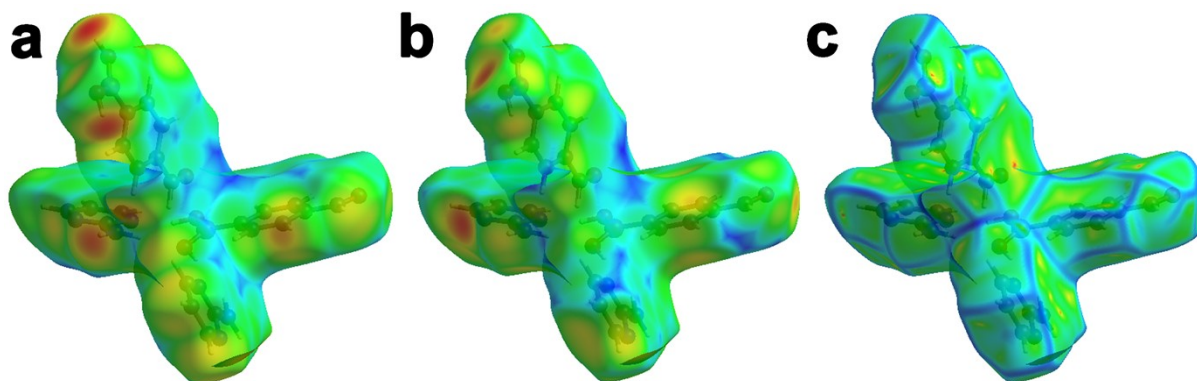
Figure S3. The 3D color mapping derived from the Hirshfeld surface analysis of **AP·FPBA** shows (a) d_i, (b) d_e, and (c) curvedness.

Table S3. Hirshfeld surface analysis of **AP·FPBA** by utilizing the 150 K SCXRD data.

Temperature	Surface Property	Range (Minimum/Maximum)	Globularity and Asphericity	Surface Volume and Area
150 K	d_i	0.6944 / 2.5139	0.647 and 0.037	584.10 Å³ and 521.22 Å²
	d_e	0.6942 / 2.5204		
	d_{norm}	-0.6645 / 1.2979		
	Shape index	-0.9948 / 0.9980		
	Curvedness	-3.6642 / 0.3540		
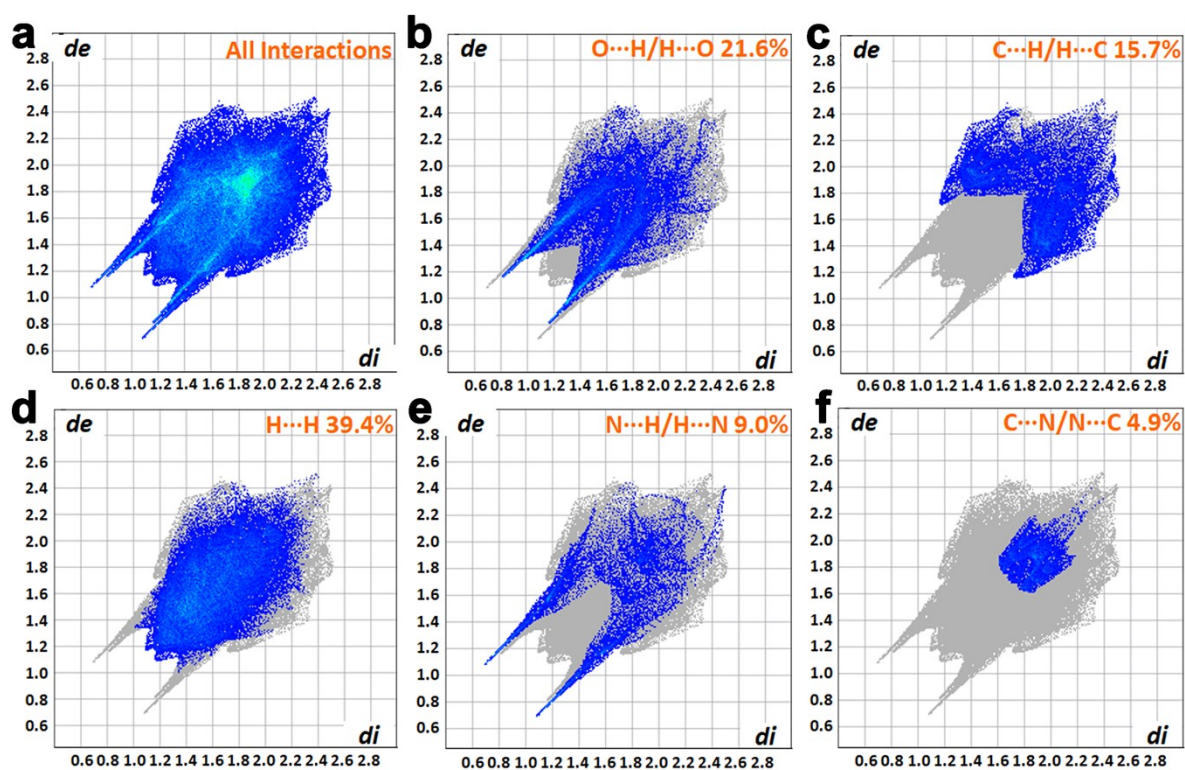
Figure S4. 2D fingerprint (d_e vs d_i) plot of **AP·FPBA** showing (a) all the possible interactions and the percentages of (b) O···H/H···O, (c) C···H/H···C, (d) H···H, (e) N···H/H···N and (f) C···N/N···C interactions in **AP·FPBA**.
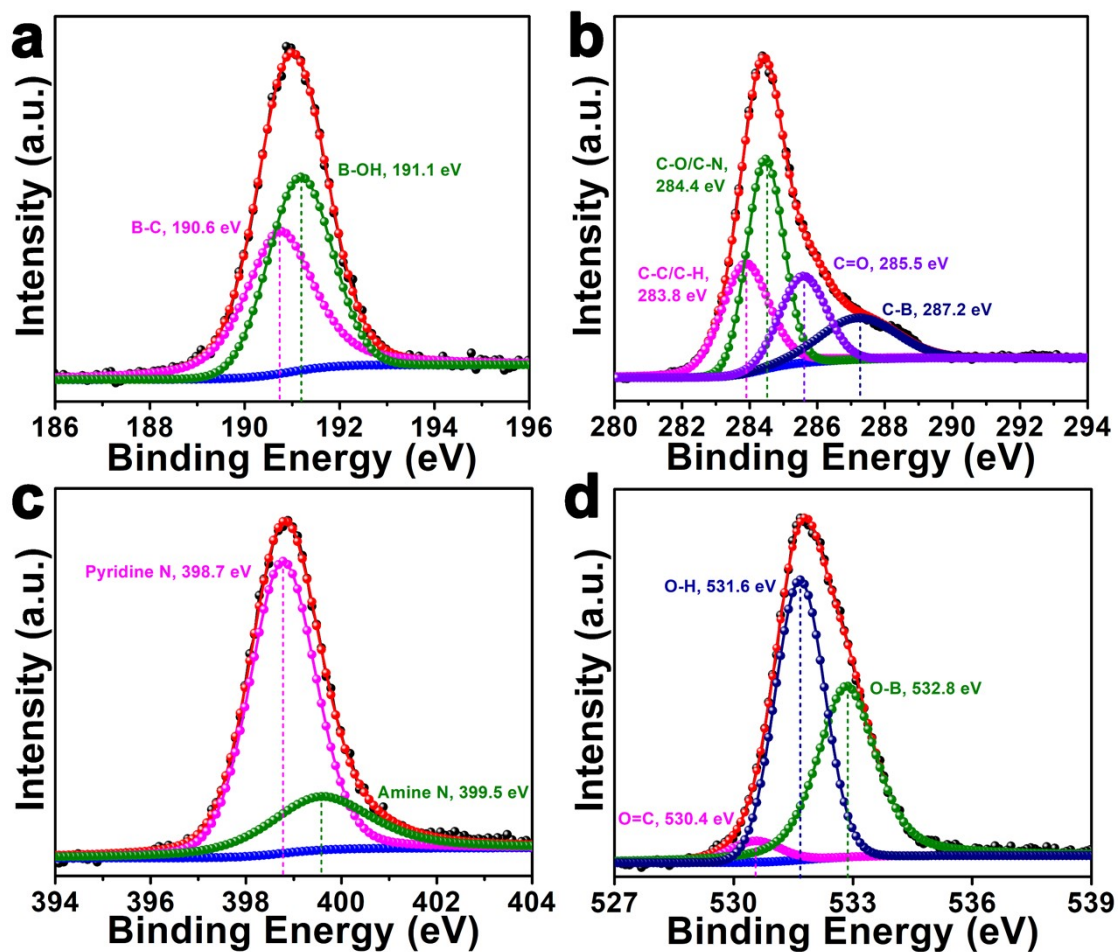
Figure S5. The X-ray photoelectron spectrum (a) B1s, (b) C1s, (c) N1s, and (d) O1s of **AP·FPBA** co-crystal.
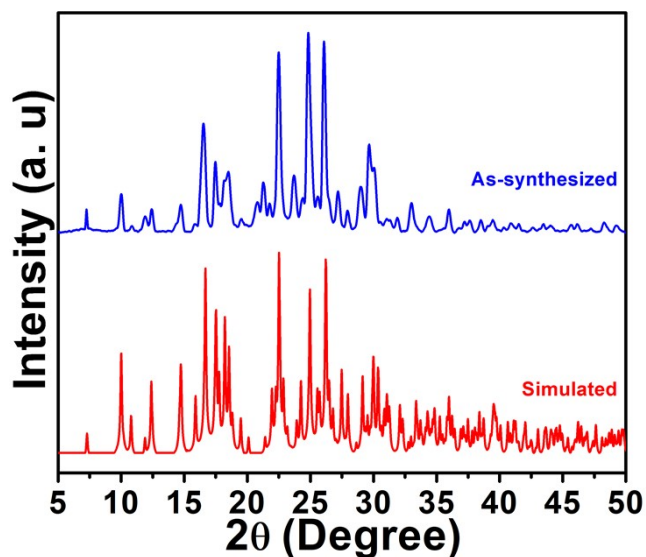
Figure S6. The room temperature powder X-ray diffraction profile of **AP·FPBA** along with its simulated profile from the 298 K SCXRD data.
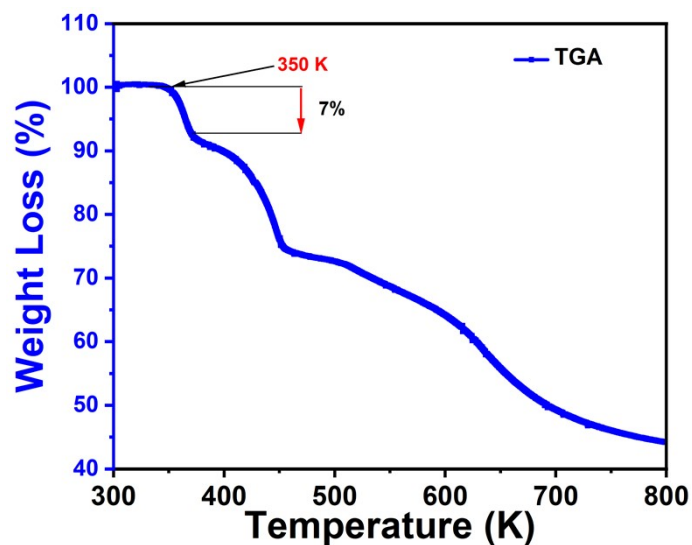
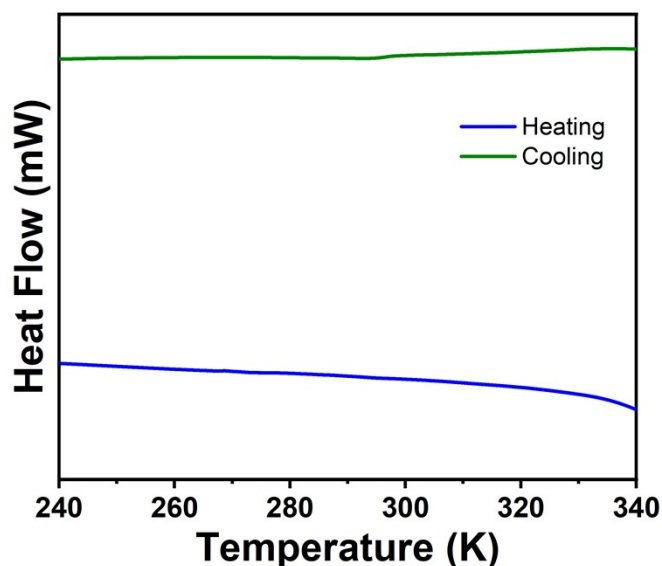**Figure S7.** The thermogravimetric analysis profile of **AP·FPBA**.

Figure S8: The DSC traces of **AP·FPBA** in the heating and cooling runs (10 °C min⁻¹).
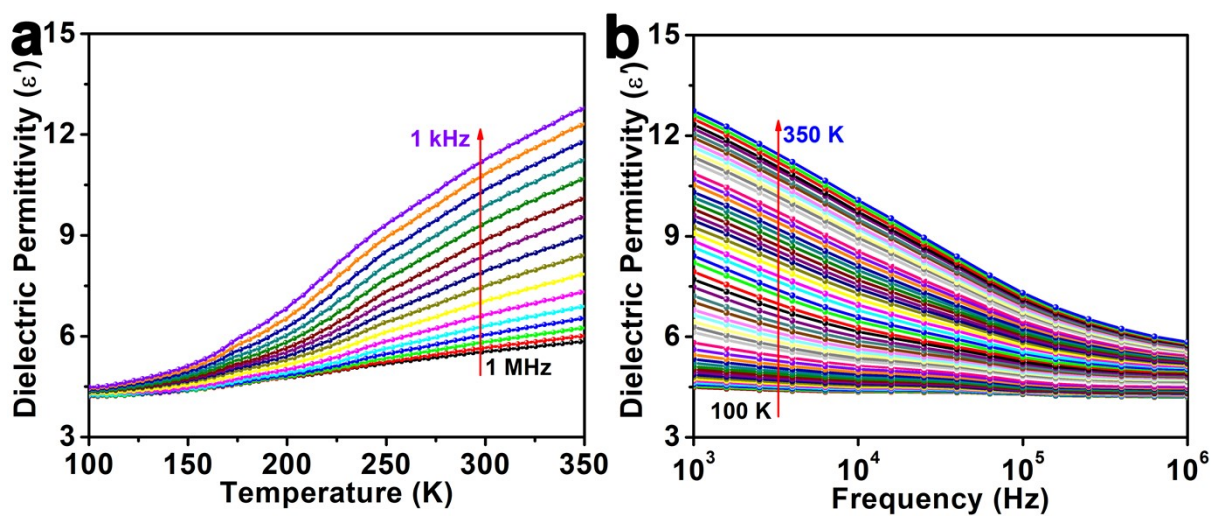
Figure S9. The (a) temperature- and (b) frequency-dependant dielectric permittivity plot of **AP·FPBA**.
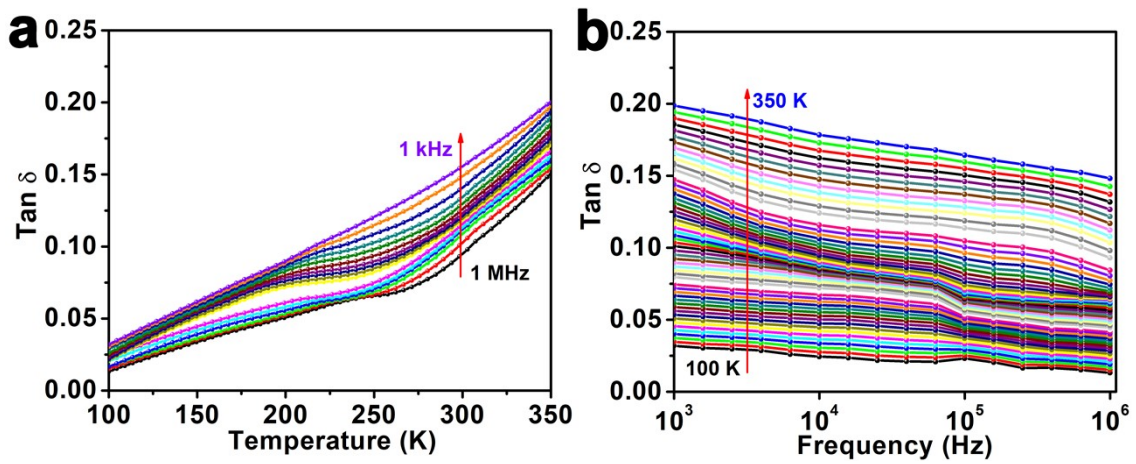
Figure S10. The (a) temperature and (b) frequency dependant dielectric loss plot of **AP·FPBA**.
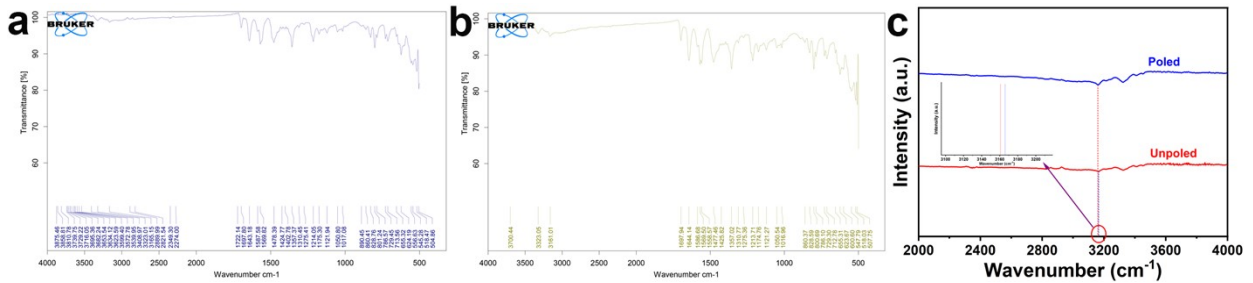
Figure S11: IR spectra profile of **AP·FPBA** a) as made sample b) poled sample c) comparison between both in the H-bonding region.
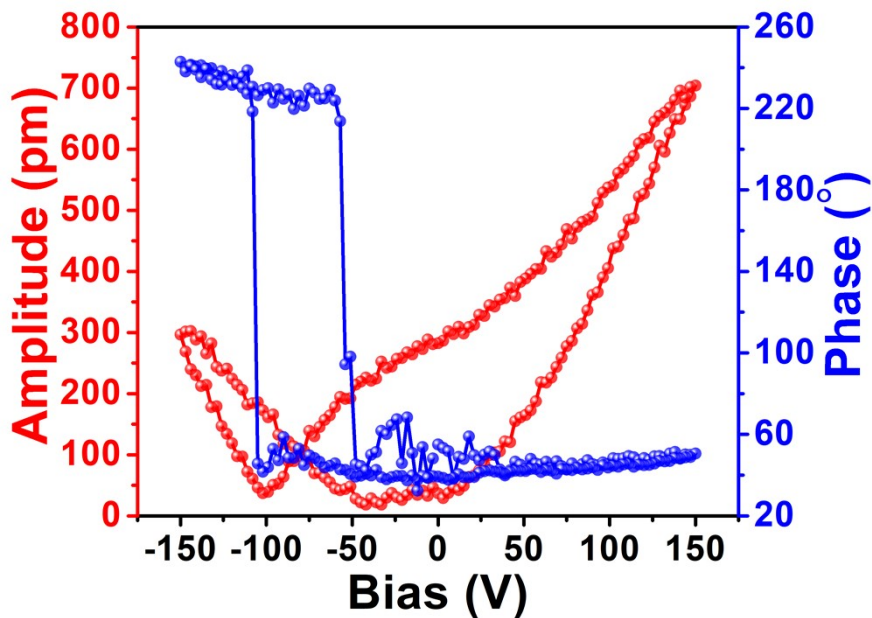
Figure S12. The off-state PFM amplitude-bias butterfly and phase-bias hysteresis loops for **AP·FPBA**.

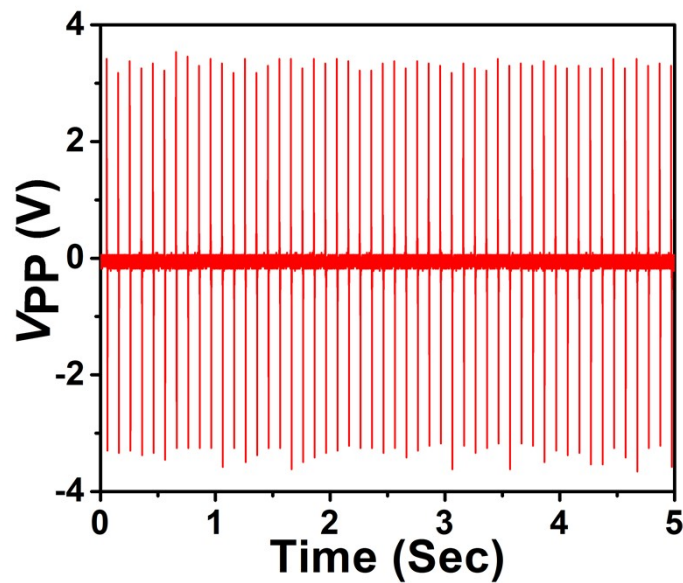**Figure S13.** d_{33} value for a poled compacted pellet of **AP·FPBA**.

Figure S14. The polarity-switching V_{PP} profile of **AP·FPBA** device.
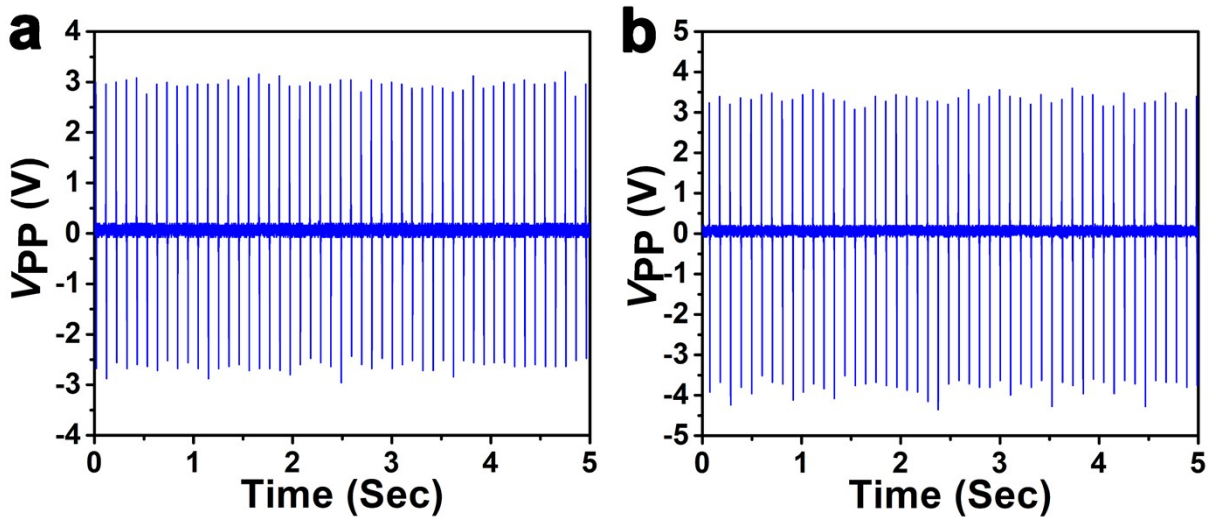

Figure S15. Open circuit peak-to-peak voltage of **AP·FPBA** on different devices.
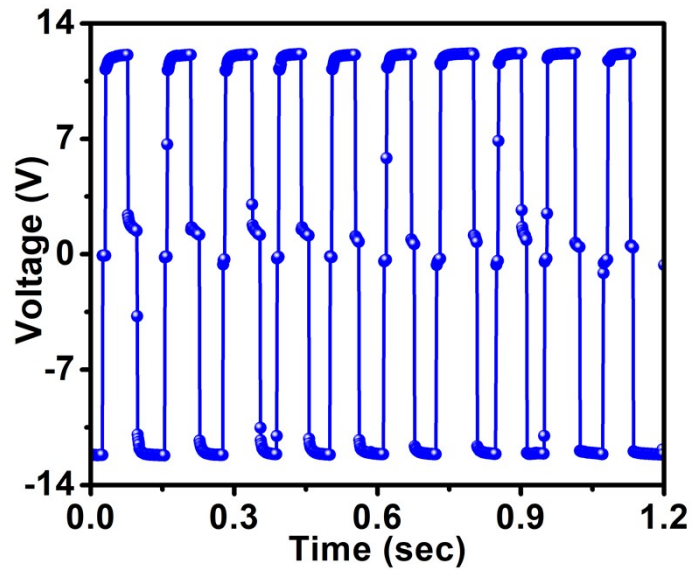
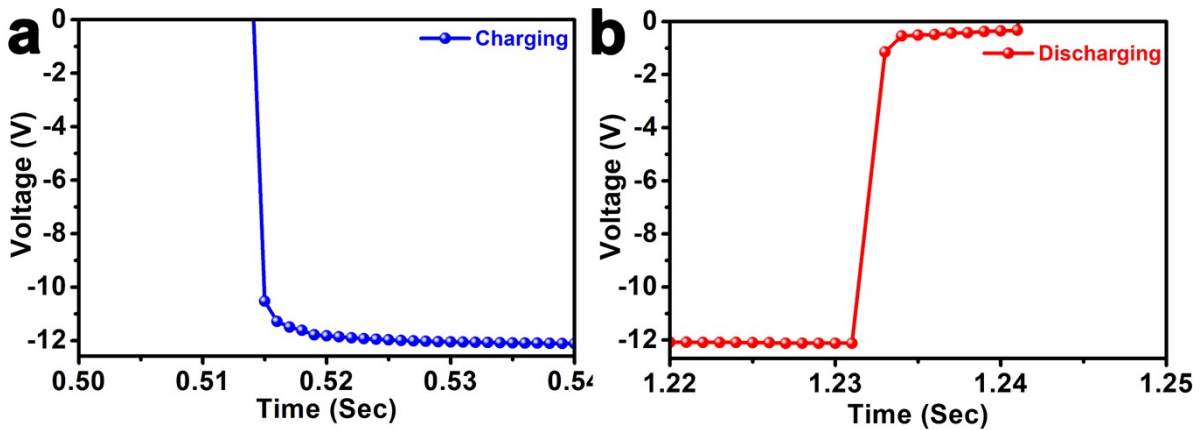**Figure S16.** The charging and discharging profile diagram **AP·FPBA**.

Figure S17. (a) The Charging profile of **AP·FPBA** with negative voltage amplitude. (b) The discharging profile of **AP·FPBA** with negative voltage amplitude.
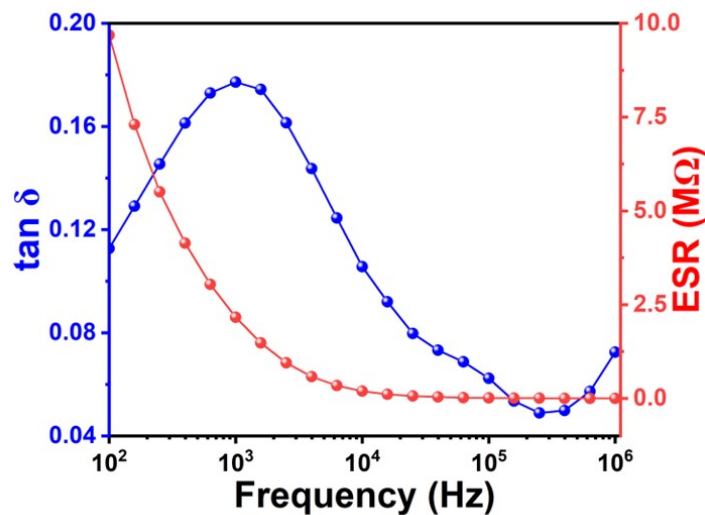

Figure S18. The left-hand plot depicts the frequency dependence of the loss tangent (tan δ), while the right-hand plot illustrates the variation of equivalent series resistance (ESR) with frequency for a 2.2 × 2.2 mm² capacitor device at 298 K.

Table S4. Comparison table for capacitor charging outcomes of **AP·FPBA** device with known devices.

Sl. No.	Compound	Capacitance	Energy density/ capacitance density	Power density ($\mu W/cm^3$)	Equivalent Series Resistance (ESR)	Charge, discharge time (s)	Active area and thickness	Ref.
1	PANI/CNF/PVA	89.9 mF	98.9 mF/cm² (Surface)		0.685 Ω at 1 kHz	79 s, 98 s		3
2	**AP·FPBA**	13.05 pF	1.52 µJ/cm³ (volumetric)	6.33 (volumetric)	2.16 MΩ at 1 kHz	0.67 s, 0.24 s	2.2 × 2.2 mm², 0.13 mm	This Work

References:

1. Sheldrick, G. M., A short history of SHELX. *Acta Crystallogr. A* **2008**, *64*, 112– 122.

2. Spek, A. L., Structure validation in chemical crystallography. *Acta Crystallogr. D* **2009**, *65*, 148– 155.

3. Anju, V.; Narayanankutty, S. K., High dielectric constant polymer nanocomposite for embedded capacitor applications. *Mater. Sci. Eng. B* **2019,** *249*, 114418.